Brain and behavioral alterations in subjects with social anxiety dominated by empathic embarrassment

Shisei Tei[a,b,c,1,2], Jukka-Pekka Kauppi[d,1], Kathryn F. Jankowski[e,1], Junya Fujino[a,f,1], Ricardo P. Monti[g], Jussi Tohka[h], Nobuhito Abe[i], Toshiya Murai[a], Hidehiko Takahashi[a,j,2], and Riitta Hari[k,2]

[a]Department of Psychiatry, Graduate School of Medicine, Kyoto University, 606-8507 Kyoto, Japan; [b]School of Human and Social Sciences, Tokyo International University, 350-1198 Saitama, Japan; [c]Institute of Applied Brain Sciences, Waseda University, 359-1192 Saitama, Japan; [d]Faculty of Information Technology, University of Jyväskylä, FI-40014 Jyväskylä, Finland; [e]Department of Psychology, University of Oregon, Eugene, OR 97403; [f]Medical Institute of Developmental Disabilities Research, Showa University, 157-8577 Tokyo, Japan; [g]Gatsby Computational Neuroscience Unit, University College London, W1T 4JG London, United Kingdom; [h]AI Virtanen Institute for Molecular Sciences, University of Eastern Finland, FI-70211 Kuopio, Finland; [i]Kokoro Research Center, Kyoto University, 606-8507 Kyoto, Japan; [j]Department of Psychiatry and Behavioral Sciences, Tokyo Medical and Dental University, 113-8510 Tokyo, Japan; and [k]Department of Art, School of Arts, Design and Architecture, Aalto University, FI-00076 Espoo, Finland

Contributed by Riitta Hari, December 31, 2019 (sent for review October 16, 2019; reviewed by Dean Mobbs and Simone G. Shamay-Tsoory)

Social-anxiety disorder involves a fear of embarrassing oneself in the presence of others. Taijin-kyofusho (TKS), a subtype common in East Asia, additionally includes a fear of embarrassing others. TKS individuals are hypersensitive to others' feelings and worry that their physical or behavioral defects humiliate others. To explore the underlying neurocognitive mechanisms, we compared TKS ratings with questionnaire-based empathic disposition, cognitive flexibility (set-shifting), and empathy-associated brain activity in 23 Japanese adults. During 3-tesla functional MRI, subjects watched video clips of badly singing people who expressed either authentic embarrassment (EMBAR) or hubristic pride (PRIDE). We expected the EMBAR singers to embarrass the viewers via emotion-sharing involving affective empathy (affEMP), and the PRIDE singers to embarrass via perspective-taking involving cognitive empathy (cogEMP). During affEMP (EMBAR > PRIDE), TKS scores correlated positively with dispositional affEMP (personal-distress dimension) and with amygdala activity. During cogEMP (EMBAR < PRIDE), TKS scores correlated negatively with cognitive flexibility and with activity of the posterior superior temporal sulcus/temporoparietal junction (pSTS/TPJ). Intersubject correlation analysis implied stronger involvement of the anterior insula, inferior frontal gyrus, and premotor cortex during affEMP than cogEMP and stronger involvement of the medial prefrontal cortex, posterior cingulate cortex, and pSTS/TPJ during cogEMP than affEMP. During cogEMP, the whole-brain functional connectivity was weaker the higher the TKS scores. The observed imbalance between affEMP and cogEMP, and the disruption of functional brain connectivity, likely deteriorate cognitive processing during embarrassing situations in persons who suffer from other-oriented social anxiety dominated by empathic embarrassment.

social anxiety | empathy | embarrassment | intersubject correlation | functional magnetic resonance imaging

Social-anxiety disorder (SAD), also called social phobia, is one of the most common psychiatric illnesses, with a 15% lifetime prevalence (1). SAD is characterized by avoidance of social interactions (2) due to fear of negative evaluation, such as embarrassing oneself in the presence of others (2, 3). Taijin-kyofusho (TKS), a subtype of SAD, additionally includes fear of embarrassing others (4), for example, making them feel uncomfortable because of the person's blushing, sweating, or trembling appearance (4). People with TKS overly imagine how they look from the perspective of others and think that their physical defects and/or socially inappropriate behaviors would offend or humiliate others (5).

Although TKS was initially described as a culturally specific SAD subtype prominent in interdependent cultures, particularly in East Asia, similar manifestations are consistently reported in independent cultures. For example, in the United States, 75% of SAD patients exhibit at least one of the five TKS symptoms related to other-oriented fear (6). TKS has recently been described in the *Diagnostic and Statistical Manual of Mental Disorders, Fifth Edition* (DSM-5) under SAD (7), which reflects its universal relevance and heterogeneous manifestations (e.g., shyness, self-criticism, and submissiveness; refs. 8–10). However, the brain basis and correlates of TKS still remain unclear (11, 12). As the fear of being negatively evaluated by others is the hallmark of social anxiety (9, 13), studying TKS as an exemplar of other-oriented anxiety might add crucial insights into the mechanisms underlying subjective experiences of social anxiety (14).

Given that persons suffering from TKS are hypersensitive to others' feelings and easily misunderstand others' perspectives (4, 5), we envisioned that TKS is associated with heightened affective empathy (affEMP; emotion-sharing via self–other overlap or

Significance

People are increasingly affected by social anxiety that includes emotional hypersensitivity and inaccurate interpretation of social encounters, and varies markedly in its subjective manifestations. We searched for insights into the underlying neurocognitive mechanisms of Taijin-kyofusho (TKS), a specific subtype of social-anxiety disorder common in East Asia and dominated by empathic or other-oriented embarrassment. We found TKS to be characterized by enhanced affective and reduced cognitive empathy. Moreover, analysis of functional MRI data—collected while subjects viewed videos of badly singing people—revealed disruption of the cognitive–empathy network, possibly obstructing flexible inference of others' perspective or augmenting maladaptive feelings of embarrassment. Our findings shed light on how altered affective and cognitive processing can contribute to the development of imaginary fears.

Author contributions: S.T., K.F.J., J.F., N.A., T.M., and H.T. designed research; S.T., J.-P.K., K.F.J., J.F., and N.A. performed research; S.T., J.-P.K., R.P.M., J.T., and R.H. contributed new reagents/analytic tools; S.T., J.-P.K., J.F., R.P.M., J.T., and R.H. analyzed data; and S.T., J.-P.K., K.F.J., J.F., R.P.M., J.T., N.A., T.M., H.T., and R.H. wrote the paper.

Reviewers: D.M., California Institute of Technology; and S.G.S.-T., University of Haifa.

The authors declare no competing interest.

Data deposition: The data processing and analytical pipeline discussed in this paper have been deposited at the University Hospital Medical Information Network (UMIN) Center, Japan (https://upload.umin.ac.jp/cgi-open-bin/icdr_e/ctr_view.cgi?recptno=R000043844). Preregistration materials, including a preanalytical plan, can be found in the Clinical Trials Registry of the UMIN Center, Japan (https://upload.umin.ac.jp/cgi-open-bin/icdr_e/ctr_view.cgi?recptno=R000043844).

[1]S.T., J.-P.K., K.F.J., and J.F. contributed equally to this work.

[2]To whom correspondence may be addressed. Email: chengctky@gmail.com, hidepsyc@tmd.ac.jp, or riitta.hari@aalto.fi.

This article contains supporting information online at https://www.pnas.org/lookup/suppl/doi:10.1073/pnas.1918081117/-/DCSupplemental.

First published February 10, 2020.

matching) that amplifies perception of others' negative feelings (15), or with reduced cognitive empathy (cogEMP; perspective-taking via self–other distinction) that hinders flexible inference of others' views and intentions that differ from one's own (16, 17). Feelings of embarrassment might excessively capture TKS subjects' attention (4, 5), and heightened affEMP might further enhance personal distress in response to others' distress or misfortunes (18). As a result, TKS subjects could readily translate the feelings of embarrassment of other people into personally experienced (empathic) embarrassment that leads to other-oriented fear.

Previous research suggests that affEMP is uniquely supported by fear-related activations in amygdala, insula, and anterior cingulate cortex (ACC) (11, 19, 20). Instead, cogEMP is supported by the ventromedial prefrontal and the orbitofrontal cortex (vmPFC/OFC) as well as by the temporoparietal junction (TPJ) and posterior superior temporal sulcus (pSTS) (15) involved in perspective-taking (via self–other distinction) and attention-shifting (15, 21). These empathy-related regions may also be associated with feelings of embarrassment (22–24). However, how such feelings are triggered and translated into other-oriented social fear warrants further investigation.

To study the neurocognitive basis of other-oriented social anxiety, we first correlated TKS level with scores of affEMP, cogEMP, and cognitive flexibility among 23 Japanese adults. We also applied the Toronto Alexithymia Scale (TAS) as a measure of altered self-awareness and emotionality, reflecting a precursor of empathic abnormalities (25). To measure cognitive flexibility (attentional set-shifting), we used the Wisconsin Card Sorting Test (*SI Appendix*) that is related to cognitive empathy (26, 27). Subsequently, we examined the relationship between the TKS scores and the strength and distribution of empathy-related functional MRI (fMRI) signals.

During fMRI recording, the subjects watched video clips of people who were singing badly and expressed for their performance either authentic embarrassment (EMBAR) or hubristic pride (PRIDE) (Fig. 1). Based on previous studies suggesting that empathic embarrassment can occur via two processes dominant in affective (bottom-up) and cognitive (top-down) domains (15, 17, 22), we expected that both singers would embarrass the viewers: the EMBAR singers via affEMP and the PRIDE singers via cogEMP. We further hypothesized that socially anxious subjects' affEMP would increase and cogEMP decrease during the viewing (for details, see the Introduction in *SI Appendix*).

Social anxiety may be associated with alterations of brain networks (28, 29), but the available brain connectivity findings are inconsistent (11, 28), either because of the variability of subject characteristics (e.g., high comorbidities and medication; refs. 8 and 30) or the diversity of the applied methods (e.g., the use of different anatomical masks). We thus conducted a fully data-driven, whole-brain functional segmentation analysis (FuSeISC) to account for interindividual differences in the brain-activation patterns (31, 32), thereby to better capture brain activity that is synchronized across subjects, while at the same time illustrating intersubject spatial variability in brain networks. We specifically tested the relationship between TKS scores and the strength of whole-brain connectivity (33).

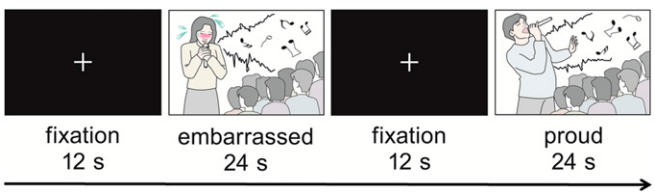

Fig. 1. fMRI task. Subjects watched video clips of five female and seven male singers singing badly in front of an audience during a singing competition. The singers acted either embarrassed or proud of their singing and expressed this via facial expression and bodily gestures. Altogether 12 blocks of video clips were presented in a pseudorandom order to each subject. Each 24-s block contained two video clips representing the same task condition (12 s each). The same video clips appeared twice through the scanning (in separate blocks). A fixation cross was displayed for 12 s between the blocks.

Table 1. Empathy-related brain activity in affEMP and cogEMP contrasts

Contrast	Brain region	MNI, *x*, *y*, *z*	*z*	Cluster size, voxels
affEMP	Right amygdala	32, −4, −28	4.41	70*
	ACC	6, 24, −8	4.80	684*
	OFC	4, 34, −14	4.63	459*
cogEMP	Right pSTS/TPJ	62, −12, 0	4.85	704*

*$P < 0.01$ (FWE-corrected).

Results

Our subjects' TKS scores ranged from 45 to 154 (mean ± SD = 80.0 ± 28.1), reflecting low-to-relatively-high TKS intensities (4, 34). The scores statistically significantly correlated positively with affEMP (personal distress: $r = 0.45$, $P = 0.048$) but not with cogEMP (perspective-taking: $r = -0.23$, $P = 0.331$) and negatively with cognitive flexibility ($r = -0.52$, $P = 0.019$; Wisconsin Card Sorting Test; *SI Appendix*).

The affEMP contrast (EMBAR > PRIDE) in general linear model (GLM)-based fMRI analyses revealed increased activity in the right amygdala and ACC ($P < 0.01$, corrected for family-wise error [FWE]; Table 1) as well as, contrary to our predictions, in OFC. The cogEMP contrast (EMBAR < PRIDE) revealed increased activity within the right pSTS/TPJ (for whole-brain analysis results, see *SI Appendix*).

Fig. 2, *Upper* shows that the activity of the right amygdala, revealed from the affEMP contrast, correlated positively with TKS scores ($r = 0.56$, $P = 0.044$; false-discovery rate [FDR] corrected for multiple comparisons), whereas the activity of the right pSTS/TPJ (Fig. 2, *Lower*), revealed from the cogEMP contrast, correlated negatively with the TKS scores ($r = -0.50$, $P = 0.048$).

The strength of ACC activity correlated positively with alexithymia scores (externally/other-oriented thinking: $r = 0.57$, $P = 0.009$), and the right pSTS/TPJ activity correlated positively with the postscan ratings of embarrassment ($r = 0.45$, $P = 0.047$; subjects watched the same video clips of the singing contest after the fMRI scanning and rated the embarrassment level for each clip; *Materials and Methods*).

Our fully data-driven, whole-brain functional segmentation analysis (FuSeISC) included computation of both the mean and the variability of intersubject correlations (ISCs) to account for interindividual differences in the brain-activation patterns (31). For the pipeline of the procedure, see Fig. 4 in *Materials and Methods*.

Fig. 3 shows statistically significant FuSeISC contrast maps separately for affEMP (upper images) and cogEMP (lower images) ($q < 0.05$, FDR-corrected for multiple comparisons). Note that the numbering and coloring of segments differs between the upper and lower images (for details, see *SI Appendix*). In the affEMP contrast (upper images), brain regions showing statistically significant involvement across subjects include the bilateral occipital cortices (segments 1, 2, and 3), bilateral premotor cortex (segment 4, also including, e.g., right anterior insula, inferior frontal gyrus, and cerebellum; see *SI Appendix*, Table S1 for a comprehensive list of all activated brain regions), superior temporal sulcus (segment 5, also including, e.g., inferior frontal gyrus and cerebellum).

In the cogEMP contrast (Fig. 3, lower images), the brain regions with statistically significant involvement include regions of

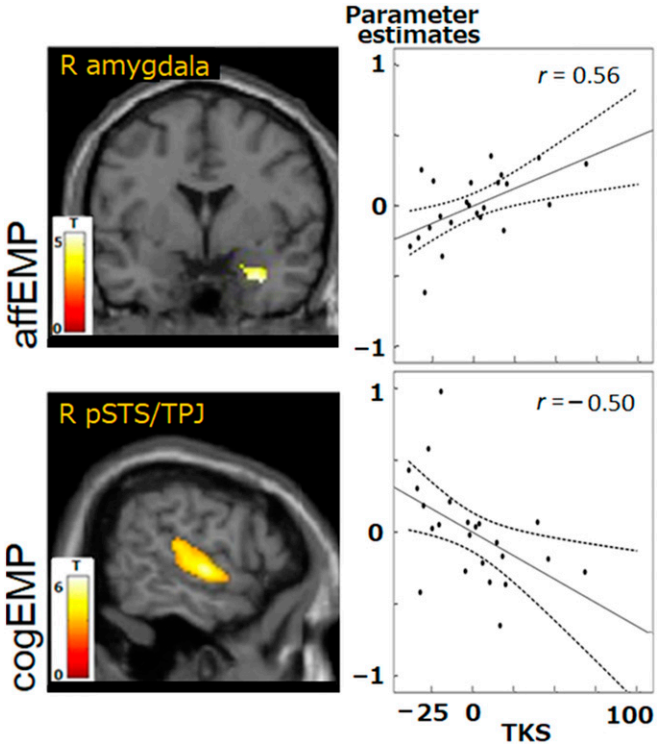

Fig. 2. Correlations between hemodynamic activity and TKS scores obtained in GLM-based analyses. During affEMP contrast (*Upper*), activity of the right amygdala increased as a function of increasing TKS scores (cluster-level $P < 0.01$, FWE-corrected). During cogEMP contrast (*Lower*), activation of the right pSTS/TPJ decreased as a function of increasing TKS scores. Dashed lines represent 95% confidence intervals. Pearson's correlation coefficients r are indicated ($P < 0.05$ after controlling for age and sex; FDR-corrected for multiple comparisons). R amygdala, right amygdala; R pSTS/TPJ, right pSTS/TPJ.

the bilateral superior temporal gyrus and pSTS/TPJ (segments 1, 2, 3, and 7), lingual gyrus (segments 4 and 9), ventral and dorsal medial prefrontal cortex (segment 5), precuneus (segment 6), and cuneus (segment 8). These segments also included multiple other brain regions, listed in *SI Appendix*, Table S1. Note that the mPFC region that we predicted to be involved in our task was not visible in the cogEMP contrast of the GLM analysis but was prominent in the FuSecISC analysis (segment 5) potentially because of its high interindividual variability (refs. 31 and 35 and Fig. 4).

In the functional connectivity analyses, the overall connectivity strength—computed in a whole-brain network comprising nodes within each of spatially isolated segment obtained from FuSeISC—correlated negatively with the TKS scores during cogEMP ($r_{\text{average}} = -0.23$, $P = 0.015$; corrected for multiple comparisons), whereas during affEMP, the correlation did not reach the statistical significance ($r_{\text{average}} = -0.14$, $P = 0.108$); see *SI Appendix* for the statistical tests.

Discussion

Our results provide both behavioral and brain-level support for the idea that other-oriented social anxiety is associated with enhanced affEMP and reduced cogEMP (5, 12, 36, 37). The negative correlation of the overall network strength with the TKS scores during cogEMP supports decreased cognitive processing in embarrassing situations, likely obstructing flexible inference of others' perspectives and attention-shifting or augmenting maladaptive feelings of embarrassment. Our results thus suggest that TKS is characterized, besides by an imbalance of affective and cognitive empathy, by disruption of the cogEMP brain network. These findings extend the current understanding of social anxiety, demonstrating how altered affEMP and cogEMP might be associated with experiences of social anxiety dominated by other-oriented imaginary fear (4, 7).

Prior studies on social anxiety have identified neural systems thought to support fear and embarrassment (11, 23), but it has remained unclear whether and how these systems might contribute to other-oriented anxiety. Here, by using naturalistic video stimuli that induced empathic embarrassment, we illuminated the behavioral and neural correlates of other-oriented anxiety in two key ways, showing that 1) TKS scores correlated positively with dispositional affEMP (personal distress) and with amygdala activity during affEMP, and 2) TKS scores correlated negatively with cognitive flexibility (attentional and perspective-shifting; refs. 15 and 38) and pSTS/TPJ activity during cogEMP. Both these results would be in line with enhanced affEMP and reduced cogEMP in other-oriented anxiety.

Stronger pSTS/TPJ activity during cogEMP than affEMP, revealed both in GLM and FuSeISC analyses, is consistent with previous research that has suggested that pSTS/TPJ subserves cogEMP via flexible shifting of attention and perspective (15, 38). This finding also converges with prior ISC studies that have highlighted the role of pSTS/TPJ in moment-to-moment cognitive appraisals via socially attuned attention (39–43). The association between pSTS/TPJ activity and the embarrassment that the viewers were feeling during cogEMP (when the singers sang badly but acted as if they were proud of their singing) also supports involvement of the pSTS/TPJ region in gaining a better understanding of others' situations in social contexts (38, 44, 45).

The reduced cogEMP in TKS, as reflected by the negative association of TKS scores with pSTS/TPJ activity, suggests that other-oriented anxiety is related to decreased ability to recognize embarrassment in social situations. This view is counterintuitive because people with social anxiety are often argued to be hypersensitive to other's feelings, especially to others' negative emotions (3, 9). However, our view aligns with the growing body of literature implying that declined social cognition can coincide with high social sensitivity in people with social anxiety (12). In other words, whereas the socially anxious people may be highly focused on others' mental states via noticing and sharing emotions of others (affEMP skills), their inferences of the social situations or perspective of others (cogEMP skills) may be highly inaccurate (12).

Accordingly, elevated affEMP (emotional sharing) can obstruct cogEMP (perspective-taking) during highly emotional situations (46). Moreover, social anxiety may be associated with difficulties in cogEMP, especially when discerning complex emotions (47). Indeed, our subjects with high TKS scores exhibited enhanced affEMP and reduced cogEMP, possibly amplifying their attention to feelings of others but hindering flexible understanding of other's social contexts (14). These subjects therefore were preoccupied with other-oriented, irrational fear (4, 7).

The results of ISC-based brain segmentation further supported the unique roles of affEMP and cogEMP in empathic embarrassment. Along with previous studies (15, 17), the ventral and dorsal mPFC, PCC/precuneus, and pSTS/TPJ were more strongly involved during cogEMP than affEMP, whereas the anterior insula, inferior frontal gyrus, premotor cortex, STS, and cerebellum were more prominently involved during affEMP than cogEMP. One potential explanation for these differences is differential involvement of mentalization (15, 17) and motor-mirroring (48) in cognitive and affective empathy.

The negative correlation between TKS scores and the strength of overall network connectivity during cogEMP further supports the notion that social anxiety may involve disruptions of cognitive, in addition to affective, processing (12, 13, 28). More research is, however, required to investigate the extent to which

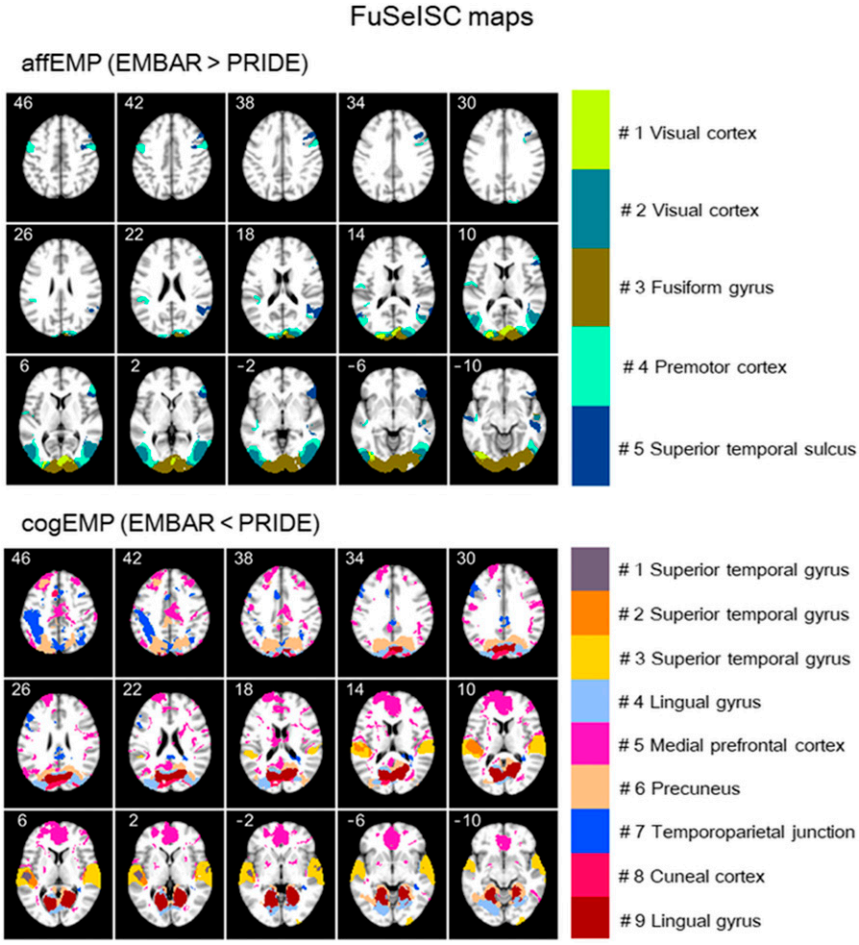

Fig. 3. ISC-based whole-brain functional segmentation. Axial FuSeISC maps are shown for the observed segments in the affEMP (*Upper*) and cogEMP (*Lower*) contrasts ($q < 0.05$, FDR-corrected), with the different segments indicated with different colors. Note that the visible (labeled) brain areas are not necessarily the only ones included in a certain segment because spatial constraints were not used in FuSeISC. MNI *z* coordinates (in millimeters) are indicated for each slice (see *SI Appendix*, Table S1 for a comprehensive list of brain regions for each segment).

these alterations can affect flexible distinction and/or balance between self–other perspectives (17, 49) or exaggerate negative perspective bias toward others, as well as toward self (e.g., misinterpreting others' impression about oneself and distorting self-image; ref. 50).

Our findings on TKS can contribute to a better understanding of the neurocognitive dysfunction of SAD, owing to the shared altered self–other awareness in both disorders (4, 5). Both TKS and SAD individuals excessively focus on others' perspectives (5). Individuals with SAD are often preoccupied with the likelihood of negative evaluation by others (51), accompanied by heightened self-awareness (12) but blurred experiences of their own emotions (47). Meanwhile, individuals with TKS are afraid of discomforting others by their physical/behavioral features (4).

The empathic embarrassment paradigm, involving self–other merging and distinction, allowed us to reveal that individuals who are more prone to other-oriented social anxiety may show enhanced affective and reduced cognitive empathy. The observed association between TKS and self-awareness scores further supports this view (*SI Appendix*), underlining the unique self–other representation in social anxiety (3, 50). In this regard, our results support the proposal that social anxiety is represented on a spectrum (9, 13), comprising diverse clinical manifestations from mild to severe and an even wider continuum of social anxiety extending into the general population, thereby affecting a multitude of interpersonal interactions (3, 50).

Limitations. The limitations of the present study include the correlational nature of our analyses, which does not inform about causal relationships between social anxiety and brain function supporting empathic involvement. Future intervention studies promoting empathy might clarify this issue. Although our study included subjects with subclinical social anxiety, some subjects' social-anxiety levels were fairly equivalent to those obtained from patients with SAD (52–54). Accordingly, manifestations of social anxiety appear to range widely from the subclinical (e.g., shyness and submissiveness) to clinical level, possibly relying on the same or overlapping dysfunctional brain mechanisms (9, 13). Nevertheless, it is essential to replicate and generalize the current findings in patients with SAD.

Although the unpredicted OFC activity observed in the affEMP contrast of the GLM analysis could reflect emotion-related processing, such as affective perspective-taking (55) and cognitive control of emotion (56), OFC is also known to be involved in cognitive flexibility (57) and cognitive empathy (27). Thus, more studies are required to further examine the role of OFC in TKS, and here event-related analysis might provide additional insights.

Notwithstanding these limitations, the present study enhances our understanding of the neural correlates of social anxiety and illustrates how data-driven brain imaging approaches (e.g., ISC) might illuminate the heterogenetic experiences of social anxiety. As our sample of 23 persons is relatively small, it would be

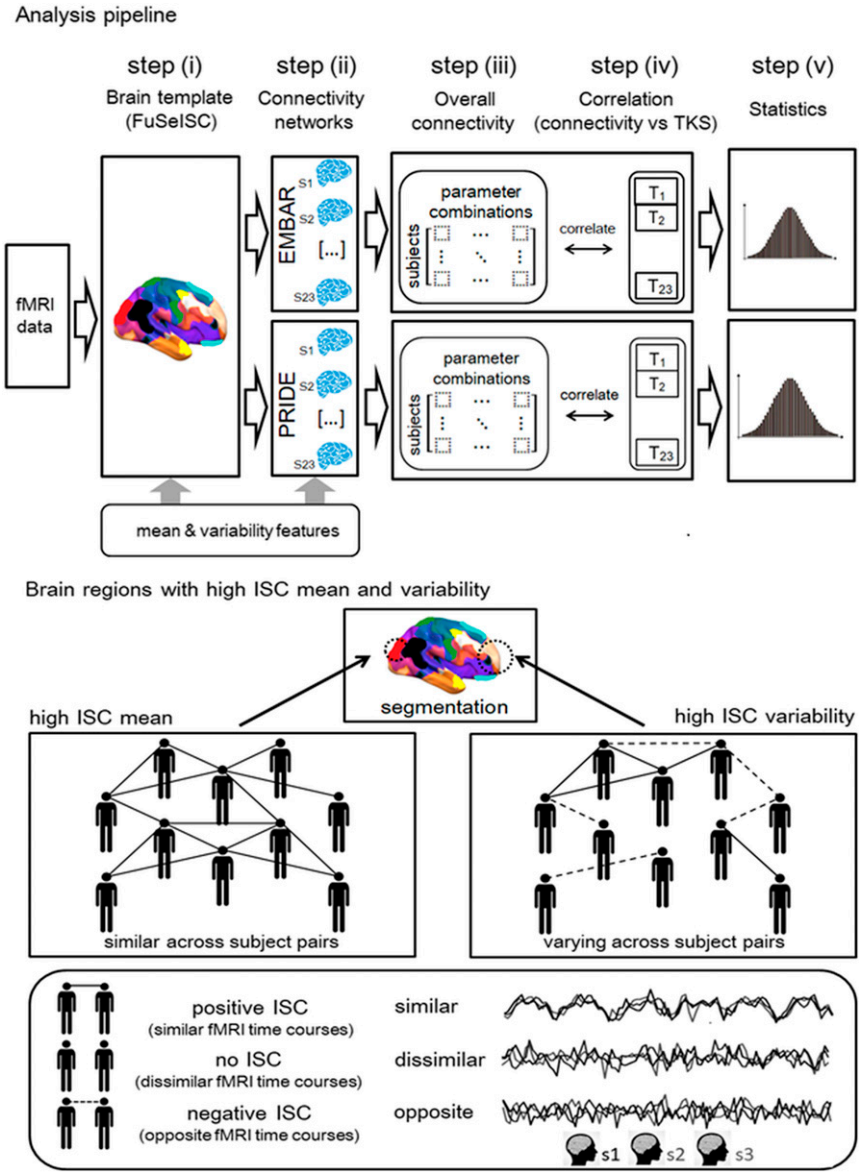

Fig. 4. Pipeline for the analysis. (*Upper*) The analysis steps of associations between TKS scores and overall brain connectivity during the empathic embarrassment task: construction of group-level brain template by FuSeISC (see *Lower* for explanation of ISC mean and variability) (i); estimation of connectivity networks for EMBAR and PRIDE (ii); computation of overall connectivity strength for each subject for multiple choices of connectivity parameters (*SI Appendix*) (iii); correlations between overall connectivity strengths and TKS scores, separately for each parameter combination (iv); and statistical evaluation of the average correlations across parameter combinations (v). (*Lower*) Concepts of ISC mean and ISC variability, used as inherent features to divide brain areas into functional segments. High mean ISC corresponds to similar fMRI time courses across multiple subject pairs (mainly positive ISCs). Meanwhile, high ISC variability corresponds to varying fMRI time courses across subject pairs, that is, similar (positive ISC), dissimilar (no ISC), and opposite (negative ISC). Some brain regions, such as early sensory areas, are typically characterized by high ISC means, whereas, for example, certain higher-order brain areas are potentially characterized by relatively high ISC variability (31).

beneficial to replicate our findings with a larger sample. To improve reproducibility and transparency, we provide the analysis code for ISC analysis at https://www.nitrc.org/projects/isc-toolbox/ (58, 59).

Conclusion. Our findings suggest that other-oriented social anxiety, here studied in subjects suffering from TKS, is characterized by an imbalance of empathy (enhanced affEMP and reduced cogEMP) as well as by disruption of the cogEMP brain network. These aberrations possibly deteriorate cognitive processing during embarrassing situations. Our results shed light on how altered affective and cognitive processing can contribute to the development of social fear.

Materials and Methods

This study was approved by the Committee on Medical Ethics of the Kyoto University and carried out in accordance with the World Medical Association's International Code of Ethics (60) and Declaration of Helsinki (61). Twenty-three subjects (16 males, 7 females; mean ± SD age, 21.3 ± 1.2 y) were recruited through an advertisement in Kyoto University and participated after written consent. Exclusion criteria included history of neurological disease, major physical/surgical illness, and substance abuse. Subjects were screened for major psychiatric disorders, including depression, schizophrenia, and bipolar disorders, with the Structured Clinical Interview for DSM-IV Axis I diagnoses, administered by experienced psychiatrists attending the Department of Psychiatry of Kyoto University. Based on the previous fMRI studies on empathy and embarrassment using a block designs and region of interest (ROI) analyses (23, 62–64), as well as sample-size determination

software G-power (65), 23 subjects were considered sufficient to detect a statistically significant ($P < 0.05$) difference ($d_z = 0.9$) (66) between conditions on a two-sided test of proportions (difference between two dependent means) with >80% power.

Behavioral Data. The conventional 31-item TKS questionnaire (4) was administered to find out how the subject differ in their TKS symptom level. This questionnaire assesses the subjects' concerns that they will do something to offend or embarrass others. The items on the questionnaire are based on clinical experience and are consistent with descriptions of the defined symptoms of TKS. The relationship between TKS scores and empathy was assessed with the Interpersonal Reactivity Index, a measure of affEMP and cogEMP, and the TAS, a measure of altered self-awareness and empathy (25, 64). The subjects' cognitive flexibility and attentional set-shifting skills (*SI Appendix*) were assessed with Wisconsin Card Sorting Test.

fMRI Task, Data Acquisition, and Analyses. Subjects watched video clips of singers who were singing badly in front of an audience during a singing competition (Fig. 1). Singers acted embarrassed or proud of their singing. These performances were designed to embarrass the viewers either via emotion-sharing (affEMP) or via perspective-taking (cogEMP). All singers presented popular Japanese songs that were familiar to our subjects. The empathic embarrassment task included two additional conditions that will be reported in a separate study (for further details, see *SI Appendix*).

The fMR images were acquired with a 3-tesla magnet equipped with a 32-channel phased-array head coil (Verio, Siemens) located at the Kokoro Research Center in Kyoto University. Functional images were obtained using a T2*-weighted gradient echoplanar imaging sequence with the following parameters: echo time (TE)/repetition time (TR), 29/2,400 ms; flip angle, 90°; field of view (FOV), 192 × 192 mm^2; matrix, 64 × 64; 38 interleaved axial slices of 3-mm thickness without gaps; resolution, 3 × 3 × 3 mm^3 voxels. Structural scans were also acquired using T1-weighted 3-dimensional magnetization-prepared rapid gradient echo sequences (TE, 3.51 ms; TR, 2,000 ms; inversion time, 990 ms; FOV, 256 × 256 mm^2; matrix, 256 × 256; resolution, 1.0 × 1.0 × 1.0 mm^3; altogether, 208 total axial sections without gaps). After completing the scanning session, subjects watched the same video clips of the singing contest outside the scanner and rated the intensity of embarrassment using a seven-point Likert scale (representing none to extreme).

Imaging data were preprocessed and analyzed using Statistical Parametric Mapping (SPM) 12 (Wellcome Department of Imaging Neuroscience). All functional brain volumes were realigned to the first volume and spatially normalized into a standard stereotactic space using a template in Montreal Neurological Institute (MNI) space. These images were resampled into 2 × 2 × 2 mm^3 voxels during the normalization process. All EPI images were smoothed using an 8-mm Gaussian kernel. Data were high pass-filtered with a time constant of 128 s.

At the single-subject level, we used a GLM in SPM and conducted *t* tests for the contrasts EMBAR > PRIDE and EMBAR < PRIDE (67). At the group level, we conducted ROI-based random-effects analyses to investigate activity specifically recruited within empathy-related brain regions. Activity within ROI masks was considered statistically significant if it survived FWE correction for multiple comparisons at the cluster level at $P < 0.01$ (primary threshold at voxel-level uncorrected, $P < 0.001$). Parameter estimates were extracted as first eigenvariates from statistically significant clusters within these a priori regions. Additionally, we report activity outside these ROIs, thresholded at the voxel-level at $P < 0.01$, with a minimum cluster extent of 50 contiguous voxels (400 mm^3) after whole-brain FWE correction for multiple comparisons. Finally, parameter estimates from the EMBAR > PRIDE and EMBAR < PRIDE contrasts were correlated with behavioral scores (Pearson's *r* correlation analyses in SPSS 22.0) after controlling for age and sex. Statistical significance was set at $P < 0.05$ (two-tailed).

FuSeISC and Connectivity Analyses. We performed data-driven FuSeISC (31) of brain regions using the ISC toolbox (59) implemented in Matlab. FuSeISC segments the whole brain directly at the group level without utilizing spatial information (such as locations, shapes, and sizes defined in the anatomical masks) but includes computation of both the mean and the variability of ISCs to account for interindividual differences in the brain-activation patterns (31, 32). Each segment is characterized by a unique pattern of ISC (31). In the current study, based on whole-brain FuSeISC, we performed condition-contrast and brain network-connectivity analyses. Fig. 4 shows the pipeline of the FuSeISC analysis from fMRI data to the statistics of correlation between TKS scores and strengths of connectivity via whole-brain segmentation (for details, see *SI Appendix*, Fig. S1).

In the connectivity analysis, nodes were defined within each of the spatially isolated segment obtained by FuSeISC, and functional networks were estimated by mixed neighborhood selection method (68). This method incorporated a random-effects component into the model, enabling the learning of both group-level and subject-specific connectivities for each node in the network. Two connectivity graphs per each subject were initially built separately, based on the time series of two conditions (EMBAR and PRIDE). From the estimated weighted connectivity graphs, we computed the overall connectivity strength for each subject (33, 69). Overall strength was obtained by calculating the median of the positive, pairwise correlation values between nodes for each subject (33). Subsequently, we examined the association between the overall connectivity strength and TKS scores across subjects during both EMBAR and PRIDE.

Data Deposition. The data processing and analytical pipeline have been deposited at the University Hospital Medical Information Network (UMIN) Center, Japan (https://upload.umin.ac.jp/cgi-open-bin/icdr_e/ctr_view.cgi?recptno=R000043844). The data discussed in this paper are available to readers upon request. Aggregated forms of data are available from S.T. Matlab code developed during the current study is also available upon reasonable request.

ACKNOWLEDGMENTS. We thank the research team of the Kokoro Research Center at Kyoto University, Japan, for their skillful assistance in data acquisition. This study was conducted using the MRI scanner and related facilities of the Kokoro Research Center. This study was supported by Grants-in-Aid for Scientific Research A (24243061, to H.T.) and on Innovative Areas (23120009 and 16H06572, to H.T.) from the Ministry of Education, Culture, Sports, Science and Technology of Japan; Grants-in-Aid for Scientific Research C (17K10326, to S.T.) and Young Scientists B (17K16398, to J.F.) from the Japan Society for the Promotion of Science, Graduate Research Opportunities Worldwide Fellowship (a component of National Science Foundation Graduate Research Fellowship 2011122786 to K.F.J.); and the Takeda Science Foundation (H.T.).

1. R. C. Kessler *et al*., The global burden of mental disorders: An update from the WHO World Mental Health (WMH) surveys. *Epidemiol. Psichiatr. Soc.* **18**, 23–33 (2009).
2. S. M. Bögels *et al*., Social anxiety disorder: Questions and answers for the DSM-V. *Depress. Anxiety* **27**, 168–189 (2010).
3. P. R. Goldin, T. Manber, S. Hakimi, T. Canli, J. J. Gross, Neural bases of social anxiety disorder: Emotional reactivity and cognitive regulation during social and physical threat. *Arch. Gen. Psychiatry* **66**, 170–180 (2009).
4. R. A. Kleinknecht, D. L. Dinnel, E. E. Kleinknecht, N. Hiruma, N. Harada, Cultural factors in social anxiety: A comparison of social phobia symptoms and Taijin kyofusho. *J. Anxiety Disord.* **11**, 157–177 (1997).
5. V. Norasakkunkit, S. Kitayama, Y. Uchida, Social anxiety and holistic cognition: Self-focused social anxiety in the united states and other-focused social anxiety in Japan. *J. Cross Cult. Psychol.* **43**, 742–757 (2012).
6. Y. Choy, F. R. Schneier, R. G. Heimberg, K. S. Oh, M. R. Liebowitz, Features of the offensive subtype of Taijin-Kyofu-Sho in US and Korean patients with DSM-IV social anxiety disorder. *Depress. Anxiety* **25**, 230–240 (2008).
7. R. G. Heimberg *et al*., Social anxiety disorder in DSM-5. *Depress. Anxiety* **31**, 472–479 (2014).
8. S. G. Hofmann, N. Heinrichs, D. A. Moscovitch, The nature and expression of social phobia: Toward a new classification. *Clin. Psychol. Rev.* **24**, 769–797 (2004).
9. M. B. Stein, D. J. Stein, Social anxiety disorder. *Lancet* **371**, 1115–1125 (2008).
10. A. J. Shackman *et al*., Neural mechanisms underlying heterogeneity in the presentation of anxious temperament. *Proc. Natl. Acad. Sci. U.S.A.* **110**, 6145–6150 (2013).
11. A. B. Brühl, A. Delsignore, K. Komossa, S. Weidt, Neuroimaging in social anxiety disorder—A meta-analytic review resulting in a new neurofunctional model. *Neurosci. Biobehav. Rev.* **47**, 260–280 (2014).
12. Y. Tibi-Elhanany, S. G. Shamay-Tsoory, Social cognition in social anxiety: First evidence for increased empathic abilities. *Isr. J. Psychiatry Relat. Sci.* **48**, 98–106 (2011).
13. S. Kajimura, T. Kochiyama, R. Nakai, N. Abe, M. Nomura, Fear of negative evaluation is associated with altered brain function in nonclinical subjects. *Psychiatry Res.* **234**, 362–368 (2015).
14. D. Mobbs *et al*., Viewpoints: Approaches to defining and investigating fear. *Nat. Neurosci.* **22**, 1205–1216 (2019).
15. S. G. Shamay-Tsoory, J. Aharon-Peretz, D. Perry, Two systems for empathy: A double dissociation between emotional and cognitive empathy in inferior frontal gyrus versus ventromedial prefrontal lesions. *Brain* **132**, 617–627 (2009).
16. C. Lamm, H. Bukowski, G. Silani, From shared to distinct self-other representations in empathy: Evidence from neurotypical function and socio-cognitive disorders. *Philos. Trans. R. Soc. Lond. B Biol. Sci.* **371**, 20150083 (2016).
17. T. Singer, C. Lamm, The social neuroscience of empathy. *Ann. N. Y. Acad. Sci.* **1156**, 81–96 (2009).

18. T. Lebra, "Shame and guilt in Japan" in *Psychological Anthropology: A Reader on Self in Culture*., R. A. LeVine, Ed. (John Wiley & Sons, 2010), pp. 102–111.
19. J. Fujino *et al*., Altered brain response to others' pain in major depressive disorder. *J. Affect. Disord.* **165**, 170–175 (2014).
20. D. Mobbs *et al*., Neural activity associated with monitoring the oscillating threat value of a tarantula. *Proc. Natl. Acad. Sci. U.S.A.* **107**, 20582–20586 (2010).
21. C. D. Frith, The social brain? *Philos. Trans. R. Soc. Lond. B Biol. Sci.* **362**, 671–678 (2007).
22. F. M. Paulus, L. Müller-Pinzler, A. Jansen, V. Gazzola, S. Krach, Mentalizing and the role of the posterior superior temporal sulcus in sharing others' embarrassment. *Cereb. Cortex* **25**, 2065–2075 (2015).
23. L. Müller-Pinzler *et al*., Neural pathways of embarrassment and their modulation by social anxiety. *Neuroimage* **119**, 252–261 (2015).
24. H. Takahashi *et al*., Brain activation associated with evaluative processes of guilt and embarrassment: An fMRI study. *Neuroimage* **23**, 967–974 (2004).
25. Y. Moriguchi *et al*., Empathy and judging other's pain: An fMRI study of alexithymia. *Cereb. Cortex* **17**, 2223–2234 (2007).
26. L. M. Grattan, R. H. Bloomer, F. X. Archambault, P. J. Eslinger, Cognitive flexibility and empathy after frontal lobe lesion. *Neuropsychiatry Neuropsychol. Behav. Neurol.* **7**, 251–259 (1994).
27. S. G. Shamay-Tsoory, R. Tomer, D. Goldsher, B. D. Berger, J. Aharon-Peretz, Impairment in cognitive and affective empathy in patients with brain lesions: Anatomical and cognitive correlates. *J. Clin. Exp. Neuropsychol.* **26**, 1113–1127 (2004).
28. C. M. Sylvester *et al*., Functional network dysfunction in anxiety and anxiety disorders. *Trends Neurosci.* **35**, 527–535 (2012).
29. X. Yang *et al*., Network analysis reveals disrupted functional brain circuitry in drug-naive social anxiety disorder. *Neuroimage* **190**, 213–223 (2019).
30. M. C. Freitas-Ferrari *et al*., Neuroimaging in social anxiety disorder: A systematic review of the literature. *Prog. Neuropsychopharmacol. Biol. Psychiatry* **34**, 565–580 (2010).
31. J. P. Kauppi, J. Pajula, J. Niemi, R. Hari, J. Tohka, Functional brain segmentation using inter-subject correlation in fMRI. *Hum. Brain Mapp.* **38**, 2643–2665 (2017).
32. M. L. Seghier, C. J. Price, Interpreting and utilising intersubject variability in brain function. *Trends Cogn. Sci.* **22**, 517–530 (2018).
33. M. N. Servaas *et al*., Connectomics and neuroticism: An altered functional network organization. *Neuropsychopharmacology* **40**, 296–304 (2015).
34. S. Tarumi, A. Ichimiya, S. Yamada, M. Umesue, T. Kuroki, Taijin Kyofusho in university students: Patterns of fear and predispositions to the offensive variant. *Transcult. Psychiatry* **41**, 533–546 (2004).
35. K. Zilles, K. Amunts, Individual variability is not noise. *Trends Cogn. Sci.* **17**, 153–155 (2013).
36. M. Gaebler, J. K. Daniels, J. P. Lamke, T. Fydrich, H. Walter, Behavioural and neural correlates of self-focused emotion regulation in social anxiety disorder. *J. Psychiatry Neurosci.* **39**, 249–258 (2014).
37. J. Shu, S. Hassell, J. Weber, K. N. Ochsner, D. Mobbs, The role of empathy in experiencing vicarious anxiety. *J. Exp. Psychol. Gen.* **146**, 1164–1188 (2017).
38. S. Tei *et al*., Collaborative roles of temporoparietal junction and dorsolateral prefrontal cortex in different types of behavioural flexibility. *Sci. Rep.* **7**, 6415 (2017).
39. R. Hari, M. V. Kujala, Brain basis of human social interaction: From concepts to brain imaging. *Physiol. Rev.* **89**, 453–479 (2009).
40. U. Hasson, A. A. Ghazanfar, B. Galantucci, S. Garrod, C. Keysers, Brain-to-brain coupling: A mechanism for creating and sharing a social world. *Trends Cogn. Sci.* **16**, 114–121 (2012).
41. L. Nummenmaa *et al*., Emotions promote social interaction by synchronizing brain activity across individuals. *Proc. Natl. Acad. Sci. U.S.A.* **109**, 9599–9604 (2012).
42. J. M. Lahnakoski *et al*., Naturalistic FMRI mapping reveals superior temporal sulcus as the hub for the distributed brain network for social perception. *Front. Hum. Neurosci.* **6**, 233 (2012).
43. S. Tei *et al*., Inter-subject correlation of temporoparietal junction activity is associated with conflict patterns during flexible decision-making. *Neurosci. Res.* **144**, 67–70 (2019).
44. P. C. Pantelis, L. Byrge, J. M. Tyszka, R. Adolphs, D. P. Kennedy, A specific hypoactivation of right temporo-parietal junction/posterior superior temporal sulcus in response to socially awkward situations in autism. *Soc. Cogn. Affect. Neurosci.* **10**, 1348–1356 (2015).
45. C. A. Hill *et al*., A causal account of the brain network computations underlying strategic social behavior. *Nat. Neurosci.* **20**, 1142–1149 (2017).
46. P. Kanske, A. Böckler, F. M. Trautwein, F. H. Parianen Lesemann, T. Singer, Are strong empathizers better mentalizers? Evidence for independence and interaction between the routes of social cognition. *Soc. Cogn. Affect. Neurosci.* **11**, 1383–1392 (2016).
47. A. S. Morrison *et al*., Empathy for positive and negative emotions in social anxiety disorder. *Behav. Res. Ther.* **87**, 232–242 (2016).
48. R. Hari, M. Sams, L. Nummenmaa, Attending to and neglecting people: Bridging neuroscience, psychology and sociology. *Philos. Trans. R. Soc. Lond. B Biol. Sci.* **371**, 20150365 (2016).
49. S. Tei *et al*., Egocentric biases and atypical generosity in autistic individuals. *Autism Res.* **12**, 1598–1608 (2019).
50. J. M. Bas-Hoogendam, H. van Steenbergen, N. J. A. van der Wee, P. M. Westenberg, Not intended, still embarrassed: Social anxiety is related to increased levels of embarrassment in response to unintentional social norm violations. *Eur. Psychiatry* **52**, 15–21 (2018).
51. M. R. Judah, D. M. Grant, N. B. Carlisle, The effects of self-focus on attentional biases in social anxiety: An ERP study. *Cogn. Affect. Behav. Neurosci.* **16**, 393–405 (2016).
52. Y. Nishikawa, J. M. Laposa, R. Regev, N. A. Rector, Social anxiety and fear of causing discomfort to others: Diagnostic specificity, symptom correlates and CBT treatment outcome. *Behav. Cogn. Psychother.* **45**, 382–400 (2017).
53. J. Kim, R. M. Rapee, J. E. Gaston, Symptoms of offensive type Taijin-Kyofusho among Australian social phobics. *Depress. Anxiety* **25**, 601–608 (2008).
54. L. Peters, Discriminant validity of the social phobia and anxiety inventory (SPAI), the social phobia scale (SPS) and the social interaction anxiety scale (SIAS). *Behav. Res. Ther.* **38**, 943–950 (2000).
55. S. G. Shamay-Tsoory, H. Harari, J. Aharon-Peretz, Y. Levkovitz, The role of the orbitofrontal cortex in affective theory of mind deficits in criminal offenders with psychopathic tendencies. *Cortex* **46**, 668–677 (2010).
56. K. N. Ochsner, J. J. Gross, The cognitive control of emotion. *Trends Cogn. Sci.* **9**, 242–249 (2005).
57. H. F. Clarke, J. W. Dalley, H. S. Crofts, T. W. Robbins, A. C. Roberts, Cognitive inflexibility after prefrontal serotonin depletion. *Science* **304**, 878–880 (2004).
58. J.-P. Kauppi, J. Pajula, J. Tohka, isc-toolbox: Inter-subject correlation analysis for fMRI in Matlab. NeuroImaging Tools and Resources Collaboratory. https://www.nitrc.org/projects/isc-toolbox/ (15 June 2015).
59. J. P. Kauppi, J. Pajula, J. Tohka, A versatile software package for inter-subject correlation based analyses of fMRI. *Front. Neuroinform.* **8**, 2 (2014).
60. World Medical Association, WMA Declaration of Helsinki – Ethical principles for medical research involving human subjects (2018). https://www.wma.net/policies-post/wma-declaration-of-helsinki-ethical-principles-for-medical-research-involving-human-subjects/. Accessed 6 November 2018.
61. World Medical Association, WMA International Code of Medical Ethics (2018). https://www.wma.net/policies-post/wma-international-code-of-medical-ethics/. Accessed 6 November 2018.
62. J. Zaki, J. Weber, N. Bolger, K. Ochsner, The neural bases of empathic accuracy. *Proc. Natl. Acad. Sci. U.S.A.* **106**, 11382–11387 (2009).
63. J. Zaki, K. Hennigan, J. Weber, K. N. Ochsner, Social cognitive conflict resolution: Contributions of domain-general and domain-specific neural systems. *J. Neurosci.* **30**, 8481–8488 (2010).
64. S. Tei *et al*., Can we predict burnout severity from empathy-related brain activity? *Transl. Psychiatry* **4**, e393 (2014).
65. F. Faul, E. Erdfelder, A. G. Lang, A. Buchner, G*Power 3: A flexible statistical power analysis program for the social, behavioral, and biomedical sciences. *Behav. Res. Methods* **39**, 175–191 (2007).
66. K. Suwabe *et al*., Rapid stimulation of human dentate gyrus function with acute mild exercise. *Proc. Natl. Acad. Sci. U.S.A.* **115**, 10487–10492 (2018).
67. L. Nummenmaa, J. Hirvonen, R. Parkkola, J. K. Hietanen, Is emotional contagion special? An fMRI study on neural systems for affective and cognitive empathy. *Neuroimage* **43**, 571–580 (2008).
68. R. P. Monti, C. Anagnostopoulos, G. Montana, Learning population and subject-specific brain connectivity networks via mixed neighborhood selection. *Ann. Appl. Stat.* **11**, 2142–2164 (2017).
69. M. Rubinov, O. Sporns, Complex network measures of brain connectivity: Uses and interpretations. *Neuroimage* **52**, 1059–1069 (2010).

Brain and behavioral alterations in subjects with social anxiety dominated by empathic embarrassment

Shisei Tei[1], Jukka-Pekka Kauppi, Kathryn F. Jankowski, Junya Fujino, Ricardo P. Monti, Jussi Tohka, Nobuhito Abe, Toshiya Murai, Hidehiko Takahashi[1], Riitta Hari[1]

[1]To whom correspondence may be addressed
Email: chengctky@gmail.com hidepsyc@tmd.ac.jp or riitta.hari@aalto.fi

This PDF file includes:

- Supplementary text
- Figures S1
- Tables S1
- SI References

www.pnas.org/cgi/doi/10.1073/pnas.1918081117

Supplementary Introduction

Our empathic embarrassment setup is based on previous studies that have suggested that empathy may involve affective (bottom-up) and cognitive (top-down) processes (1-3); such that the perceiver would (a) resonate an emotion in the social target via a more dominant affective route (self–other matching) or (b) recognize her own emotion that differs from an emotion in the social target via a more dominant cognitive route (self–other distinction) (2, 4). Accordingly, when an individual encounters a person whose behavior is embarrassing, this individual may empathically acknowledge the situation in two ways, both by sharing the emotion with the person who is embarrassed of herself and aware of her feeling, and by not sharing the emotion with the person whose behavior is embarrassing but this person is unaware of her embarrassment (3).

On this basis, we hypothesized that the EMBAR singers would embarrass the viewer dominantly via affEMP (so that the viewer would share embarrassment with the EMBAR singer) and the PRIDE singers dominantly via cogEMP (so that the viewer would acknowledge the embarrassment of the PRIDE singer). We also predicted that PRIDE singers would trigger stronger cogEMP than affEMP because understanding the embarrassment in a situational context demands dissociating from the PRIDE singer's proud feeling.

Supplementary Methods

Behavioral data

Empathic disposition was assessed using the 28-item Interpersonal Reactivity Index (IRI), which is one of the most widely used self-report measures of dispositional empathy (5). The subscales of personal distress (PD: self-oriented feelings of anxiety and discomfort) and empathic concern (EC: feelings of compassion and concern for others) scores assessed the affective components of empathy, whereas, perspective taking (PT: adopting others' psychological point of view) assessed the cognitive component of empathy (1). Based on previous studies, the fantasy subscale was excluded (6). We assessed subjects' alexithymia level using the 20-item Toronto Alexithymia Scale (TAS-20) (7). Alexithymia represents lack of self-awareness (7), which is a proposed precursor for empathic abnormalities (6, 8). This measure yields three subscales: difficulty in identifying feelings, difficulty in describing feelings, and externally-oriented thinking. In addition, intelligence quotient (IQ) scores were estimated using a Japanese version of the National Adult Reading Test (JART; mean = 104.6 ± 8.35), based on findings from a previous study that demonstrated that JART scores successfully predicted full-scale IQ scores on the Wechsler Adult Intelligence Scale-Revised (9).

We used the Wisconsin Card Sorting Test (WCST), a well-established measure of cognitive flexibility and attentional set-shifting (10), to assess subjects' abilities to switch attention and perspectives. These abilities are crucial for cognitive perspective taking that requires individuals to compare and contrast their own perspectives with those of other people (11, 12). We adopted a computerized version of the WCST (13) where four stimulus cards were displayed on the computer screen. The cards varied according to three perceptual categories: number, color, and shape. Subjects were instructed to select one of the four cards that fit a given perceptual category but they were not told which perceptual category to use. After each card selection, subjects received feedback ('Correct' or 'Incorrect'). The perceptual category used to organize the cards shifted among these three categories during the test until subjects had

selected all 48 cards. We focused on the number of categories achieved (CAs). One CA represented one rule attainment, involving six consecutive correct card selections after a rule change. Therefore, larger CA numbers represented a greater ability to switch attention and decision rules (perspectives) (11). One subject's WCST data were omitted because of a technical error.

fMRI task, data acquisition, and analyses

Subjects watched video clips of female and male singers who were singing badly in front of an audience during a singing competition (Fig. 1). Singers acted embarrassed or proud of their singing [authentic embarrassment (EMBAR) and hubristic pride (PRIDE), respectively]. These performances were designed to embarrass the viewers either via emotion sharing [i.e. affective empathy (affEMP) with EMBAR singers] or via perspective taking [i.e. cognitive empathy (cogEMP) for PRIDE singers]. The setup also included no-singing video clips (singers neither sang nor expressed emotions and listened to instrumental background music) as well as authentic pride video clips (talented singers sang well and expressed proud of their performance). These conditions, comprising six blocks each, similar to EMBAR and PRIDE conditions, will be analyzed using a theoretically and methodologically distinct approach and reported in a separate study.

At single-subject level, we used a GLM in SPM and conducted two *t*-tests for the contrasts EMBAR > PRIDE and EMBAR < PRIDE. The design matrix included task conditions and six movement parameters (three displacements and three rotations). At group level, we conducted ROI-based random-effects analyses to investigate activity specifically recruited within empathy-related brain regions. We selected *a priori* regions that are crucially involved in affective and emotional processing, including e.g. vicarious pain (2). These ROIs included the amygdala, ACC, insula, and vmPFC/OFC. These ROI masks were generated using the Automatic Anatomical Labeling atlas as implemented in the WFU pickatlas toolbox (14). We limited our analysis to the right hemisphere, given that right-hemisphere-dominant brain activity within these hypothesized regions is commonly reported in studies of social cognition (15). Activity within ROI masks was considered statistically significant if it survived FWE correction for multiple comparisons at a cluster-level of $p < 0.01$ (primary threshold at voxel-level uncorrected, $p < 0.001$). Parameter estimates were extracted as first eigenvariates from statistically significant clusters within these *a priori* regions. We also included an ROI in the right pSTS/TPJ likely supporting in cogEMP (16-18). We examined these regions as a single/unified region, in accordance with previous studies (16, 19, 20). Per our previous approach (6), pSTS/TPJ parameter estimates were extracted from a cluster obtained from a whole-brain analysis. Additionally, we reported activity outside these ROIs thresholded at voxel-level $p < 0.01$ with a minimum cluster extent of 50 contiguous voxels after whole-brain FWE correction for multiple comparisons. To locate and interpret the anatomical location of these clusters, we consulted MRIcron (http://people.cas.sc.edu/rorden/mricron/index.html), the Talairach Daemon database (http://www.talairach.org), and neuroanatomy atlases. Finally, parameter estimates from the affEMP and cogEMP contrasts were correlated with behavioral scores using Pearson's *r* correlation analyses in SPSS 22.0 (Chicago, IL, USA), after controlling for age and gender. Statistical significance was set at $p < 0.05$ (two-tailed).

FuSeISC (ISC-based functional segmentation) and connectivity analysis

Overview

In addition to the GLM-based analyses, we conducted data-driven analyses based on ISCs (21). While GLM parameter estimates indicate the strength of brain activity, ISC quantifies the strength of the *similarity* of brain activity time-series across subjects [i.e., similar synchronization of fMRI time courses to the stimulus timing in all subject pairs; note that we call this effect synchronization although the signals were measured from different individuals sequentially (22, 23)]. Recently, the conventional voxel-wise ISC method has been extended to locate stimulus-induced inter-regional correlations between brains exposed to the same stimuli (24), as well as to identify functional segments and networks of brain areas involved in processing the stimuli (21, 25). FuSeISC segments the whole-brain directly in group-level analysis without utilizing spatial information (e.g., locations, shapes, and sizes defined in the anatomical masks), dividing the brain into multiple segments associated with different ISC patterns across multiple conditions. After computing the whole-brain segmentation, we performed two analyses based on it. First, we inspected segments showing statistically significant differences in the strength of ISC during EMBAR and PRIDE conditions. Second, we constructed overall (whole-brain) functional networks for each subject using the mixed neighborhood selection method and studied the association between the strength of overall connectivity and TKS scores. Figure 4 shows the pipeline of the FuSeISC analysis from fMRI data to the statistics of correlation between TKS scores and strengths of connectivity via whole-brain segmentation.

Consideration of inter-subject variability was important in the present study because previous research has shown that social anxiety is highly heterogeneous in its manifestations (26, 27). Thus using both the mean and the variability of ISC across subjects (28, 29) might be useful in the study of the brain bases of social anxiety. FuSeISC can complement standard averaging approaches in group analyses and may enrich the conclusions (28). Both the FuSeISC and mixed neighborhood selection connectivity methods accounted for the inter-subject variability while examining empathy-related brain activity. In FuSeISC analysis, synchronization across subjects in a specific voxel was measured in terms of both the mean and variability of subject-pairwise ISC (21). In the connectivity analysis, the mixed neighborhood selection incorporated a random-effect component into the model, thereby allowing the model to learn both group-level and subject-specific connectivities for each node in the network. The purpose of using mixed neighborhood selection was to accurately recover subject-specific functional connectivity networks while sharing information across subjects in a judicious manner.

Construction of whole-brain FuSeISC maps

First, to construct a whole-brain functional segmentation (21), a correlation between fMRI time-series of each subject pair (N = 23 subjects) was computed for each voxel and task condition. Next, two ISC features (mean and variability) were extracted from the correlation matrices of each task condition. Finally, in the segmentation step, these voxels were clustered across the brain as described in (21) using the Gaussian mixture model and mutual nearest-neighbor graph-based initialization of the cluster centroids. Figure S1 shows the constructed FuSeISC map.

Construction of FuSeISC condition-contrast maps

The final number of clusters (segments) in the FuSeISC map depends on the selected neighborhood parameter *k* of the initialization algorithm. A previous study (21) showed that the total number of segments stabilized for two different task-based fMRI datasets when *k* ranged from 230 to 250. Thus, in the contrast analysis, we analyzed FuSeISC map with k = 250 (leading to 25 segments). Following the previous study (21), we removed as a post-processing step segments located predominantly in the white matter, ventricles, and the brain stem. This post-processing was important to allow better comparison with the GLM-based analysis.

Subsequently, we examined differences between EMBAR and PRIDE conditions within each segment. We first computed mean time-series within each functional segment for each subject (both for EMBAR and PRIDE conditions). Then, to find ISC differences between conditions for each segment, we used a similar procedure as described in our previous study (30) for voxel-level analysis. We first computed subject-pairwise modified Pearson-Filon statistics based on Fisher's z-transformation (ZPF), which is a recommended measure for evaluating if two non-overlapping but dependent correlation coefficients differ (31). Then, we computed a group-level statistic by taking a sum across the subject-pairwise ZPF values and conducting a permutation test on this sum ZPF statistic. We performed the test under the null hypothesis that each subject-pairwise ZPF value is drawn from a distribution with a zero mean, which would occur when there is no ISC difference between conditions. We approximated a permutation distribution by randomly flipping the sign of ZPF values before calculating the sum ZPF statistic, using a subsample of size 100'000 of all possible random labeling. We corrected the obtained *p*-values using a false discovery rate (FDR) based on the Benjamini-Hochberg procedure (32). Statistical significance was set at $q < 0.05$, FDR-corrected.

Functional connectivity analysis

We estimated brain connectivity networks from the segments obtained in FuSeISC analysis. Subsequently, we examined a linear association between subjects' TKS scores and the strength of functional connectivity in the whole brain. We employed mixed neighborhood selection to estimate functional connectivity networks (33). This method is preferred to traditional functional connectivity algorithms as it explicitly accounts for inter-subject variability, which is of primary interest in this work and has been widely reported (28, 29, 34, 35). Mixed neighborhood selection shares information across subjects via the use of a novel covariance model (36). Specifically, mixed neighborhood selection introduces a random effect

component in the neighborhood selection model, thereby learning both group-level and subject-specific connectivities for each node in the network. Such an introduction thereby allows mixed neighborhood selection to learn a richer model of functional connectivity, where the edge between any pair of regions can be seen as the sum of a *population* edge together with a *subject-specific* edge. Furthermore, mixed neighborhood selection introduces L1 sparsity constraints in order to learn parsimonious and interpretable models of functional connectivity. Parameter inference proceeds by maximizing the penalized complete-data log-likelihood of the form:

$$L_c^{\lambda_1,\lambda_2}(\phi^v) = L_c\,(\phi^v) + \lambda_1\|\beta^v\|_1 + \lambda_2\|\sigma^v\|_1,$$

where $L_c(\phi^v)$ is the negative log-likelihood, and $\phi^v = (\beta^v, \sigma^v)$ are model parameters for node v to be estimated.

An objective of this form is to separately optimize each node in the network. Regularization parameters λ_1 and λ_2 are user parameters selected before estimating the model: λ_1 enforces sparsity for edges of the graph at the population level, and λ_2 shrinks standard deviation terms σ^v of the random effects component. Large values of λ_1 will lead to sparse networks at the population level, and large values of λ_2 will penalize the variance of the random effects, leading to sparse subject-specific contributions. In the context of high-dimensional data, regularization is fundamental, as it reduces the total number of free parameters, thereby making estimation feasible from an optimization perspective. We note that without regularization, the parameters are not identifiable, i.e., there are an infinite number of possible solutions. For the estimation of the models, we used the expectation-maximization algorithm (33) implemented in the statistical software R (37) (https://www.r-project.org).

To define nodes of the functional network, we used brain-wide segments obtained by FuSeISC as volumes of interest (VOIs). First, to specify each spatially isolated segment as one independent VOI, we re-labeled all the original FuSeISC-revealed segments. This procedure was done because these segments contained spatially separated subsegments that were initially labeled as the same segment (i.e., identically colored segment in the FuSeISC maps). With this re-labeling, these subsegments were treated as different (independent) VOIs. Second, to estimate the functional networks by mixed neighborhood selection method (33), these VOIs were thresholded at a minimum cluster extent of 500 contiguous voxels (38). Then, mean fMRI time-series were extracted from each VOI for each subject and used in the network estimation stage. Two connectivity graphs per each subject were separately built based on the time-series of two conditions (EMBAR and PRIDE). From the estimated weighted connectivity graphs, we computed the whole-brain (overall) connectivity strength for each subject. Following the procedure used in a prior study (39), the whole-brain connectivity strength was obtained by calculating the median of the positive, pairwise correlation values between the nodes for each subject. Subsequently, a correlation coefficient was computed between the whole-brain connectivity strength and TKS scores across subjects (39) during the affEMP and cogEMP conditions. The correlation coefficient depends on selected parameters (40); thus, to alleviate any biases, we assessed the statistical significance of the average correlation coefficient, based on multiple brain networks that were constructed with different hyper-parameter combinations (see Fig. 4). In the context of the regularization parameters, λ_1 and λ_2, this can be interpreted as performing Bayesian model averaging (41). In the current study, the following parameters were used: λ_1 = [0.05, 0.1, 0.2], λ_2 = [0.01, 0.02] and k = [150, 200, 250, 300], leading to 3*2*4 = 24

brain networks per subject with a different numbers of nodes (61, 51, 43, 41, depending on k) and sparsity levels (depending on λ_1, λ_2). Thus, we computed 24 (dependent) correlation coefficient values, one per each network, and averaged them. To assess the statistical significance of this average correlation coefficient, we estimated p-values by conducting an approximate randomization test, where the null distribution was formed by computing the corresponding mean correlation coefficient after randomly shuffling the TKS-score vector 10'000 times.

Supplementary Results and Discussion

Behavioral data

As intended by our study design, subjects' post-scan embarrassment ratings of the singing video clips were not statistically significantly different between the EMBAR and PRIDE conditions (21.8 ± 10.6 versus 20.2 ± 11.1; n.s.), which suggested that subjects experienced fairly similar level of empathic embarrassment in EMBAR and PRIDE. TKS scores correlated positively with personal-distress subscale of IRI ($r = 0.45$, $p = 0.048$), but not with perspective taking and empathic concern ($r = -0.23$, $p = 0.331$, and $r = -0.29$, $p = 0.230$, respectively). As an additional analysis, we examined the relationship between subjects' level of TKS and alexithymia (measured by TAS questionnaire). The results showed that TKS scores correlated positively with the difficulty of identifying feelings ($r = 0.49$, $p = 0.029$) but not with the difficulty of describing feelings ($r = 0.30$, $p = 0.205$) or with externally-oriented thinking ($r = -0.09$, $p = 0.716$).

Neuroimaging data

In the whole-brain GLM analysis, affEMP contrast revealed statistically significant activity within the left occipital cortex [MNI: −22, −82, 6; cluster = 195; Z= 6.40] and right occipital cortex [MNI: 30, −70, 4; cluster = 245; Z= 5.90], thresholded at $p < 0.01$ with a minimum cluster extent of 50 contiguous voxels after whole-brain correction for multiple comparisons. The cogEMP contrast did not reveal any statistically significant activity. Furthermore, in the ROI analysis, insula and inferior frontal gyrus (IFG) activity in the affEMP contrast, as well as MPFC activity in the cogEMP contrast did not survive our statistical threshold. The TKS level did not correlate with ACC or MPFC obtained from the affEMP contrast ($r = 0.23$, $p = 0.33$ and $r = 0.32$, $p = 0.16$, respectively). Whether ACC, insula, IFG and MPFC are essentially involved in the feature of TKS remains the topic of future studies.

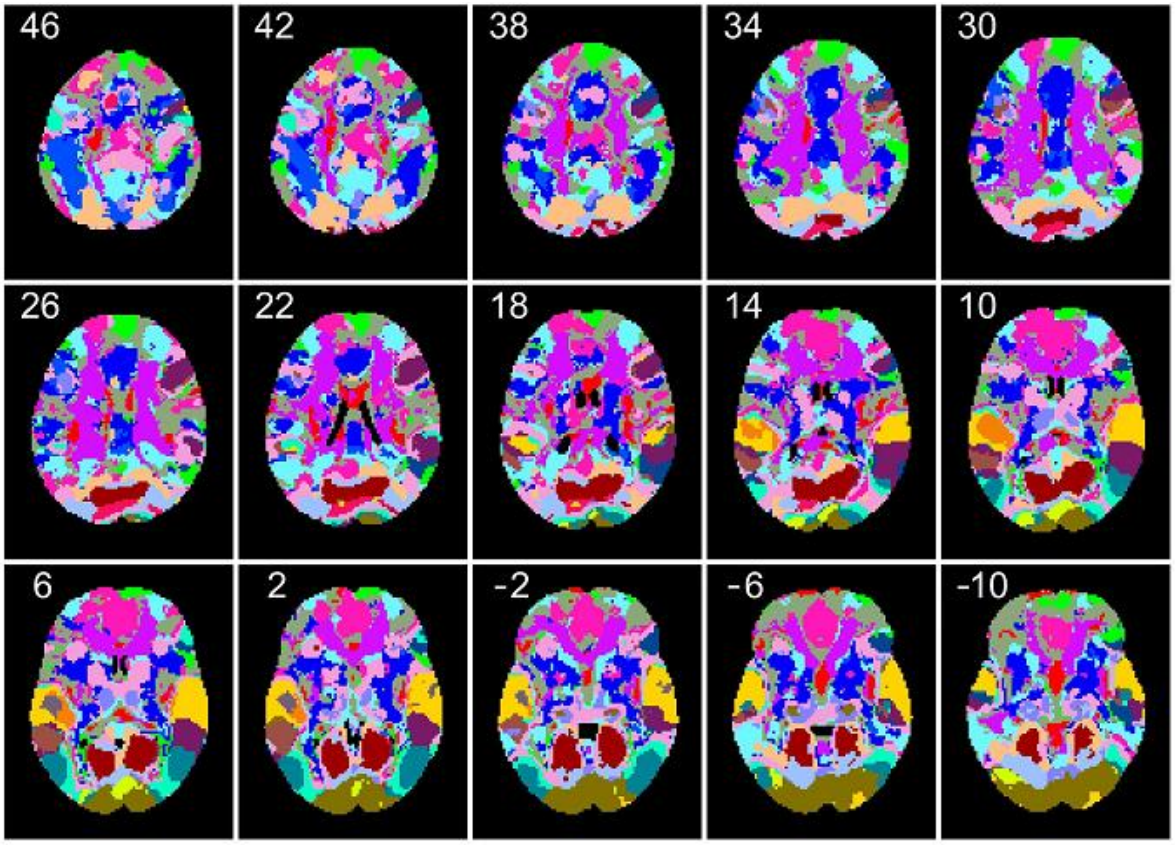

Fig. S1 whole-brain FuSeISC map

FuSeISC map during the empathic embarrassment task ($q < 0.05$, FDR-corrected). Montreal Neurological Institute (MNI) z-coordinates (in mm) are shown for each axial slice. Each colored segment corresponds to a unique pattern of ISC across subjects. This map was used as the template for contrast and connectivity analyses.

Table S1 MNI coordinates for the FuSeISC segments

The affEMP contrast revealed five segments and the cogEMP contrast nine. Each segment contained multiple "subsegments" that were spatially separated from each other. For example, in affEMP contrast, the first segment (#1) contained three subsegments.

affEMP contrast

Segment (size in voxels)	Brain Regions		MNI	Sum ZPF statistic
1 (824)	visual cortex	L	−4 −88 8	172.14
	fusiform gyrus	R	36 −78 −12	
	visual cortex	R	22 −96 10	
2 (2692)	visual cortex	L	−38 −76 6	158.02
	visual cortex	R	48 −74 2	
	precentral gyrus	L	−48 2 50	
	superior temporal gyrus	L	−54 −16 −8	
3 (6817)	lingual gyrus	L	−6 −86 −6	100.27
	middle temporal gyrus	L	−54 2 −16	
	fusiform gyrus	R	40 −48 −22	
4 (3483)	visual cortex	L	−8 −76 6	68.10
	premotor cortex	R	50 −2 46	
	premotor cortex	L	−52 2 44	
	cerebellum	R	24 −64 −54	
	inferior frontal gyrus/anterior insula	L	−54 34 6	
	superior temporal gyrus	R	46 −36 22	
	somatosensory cortex	R	56 −10 10	
	superior temporal gyrus	R	46 −24 −4	
	cerebellum	R	26 −60 −26	
5 (3150)	superior temporal gyrus	L	−52 −2 −8	36.94
	cerebellum	R	20 −78 −34	
	frontal eye field	L	−46 18 38	
	superior temporal sulcus	R	58 −12 −12	
	premotor cortex	L	−8 18 62	
	premotor cortex	L	−38 0 44	
	associative visual cortex	R	56 −62 14	

cogEMP contrast

Segment (size in voxels)	Brain Regions		MNI	Sum ZPF statistic
1 (259)	superior temporal gyrus	R	52 −18 2	277.62
	superior temporal gyrus	L	−62 −8 0	
2 (679)	superior temporal gyrus	R	46 −24 8	199.20
	superior temporal gyrus	L	−44 −20 6	
3 (4807)	superior temporal gyrus	L	−58 −14 2	75.91
	superior temporal gyrus	R	56 −18 2	
	visual cortex	L	−30 −94 −8	
4 (5093)	lingual gyrus	R	4 −72 6	61.31
	superior temporal sulcus	L	−46 −2 −8	
	inferior parietal lobule	L	−34 −56 48	
5 (13764)	ventromedial prefrontal cortex	R	10 44 14	58.11
	precentral gyrus	L	−24 −8 40	
	temporoparietal junction	R	44 −64 32	
	posterior cingulate cortex	R	6 −52 22	
	postcentral gyrus	R	52 −8 34	
	planum temporale	R	36 −36 12	
	cerebellum	L	−48 −58 −46	
	motor cortex	R	54 −4 10	
	lateral occipital cortex	L	−30 −74 10	
	fusiform gyrus	L	−56 −50 −12	
	temporoparietal junction	R	64 −32 30	
	inferior temporal gyrus	R	56 −30 −22	
	putamen	L	−24 4 −4	
	cerebellum	R	14 −50 −18	
	superior frontal gyrus	L	−22 54 −6	
	cerebellum	L	−36 −84 −36	

cogEMP contrast, continued

Segment (size in voxels)	Brain Regions		MNI	Sum ZPF statistic
6 (7747)	precuneus	L/R	0 −56 14	56.42
	middle frontal gyrus	R	26 30 46	
	visual cortex	R	32 −82 14	
	cerebellum	R	14 −44 −48	
7 (7372)	motor cortex	R	38 −26 54	55.90
	motor cortex	R	2 8 48	
	temporoparietal junction	L	−38 −60 48	
	precuneus	L/R	0 −70 48	
	middle frontal gyrus	L	−36 8 56	
	inferior frontal gyrus	R	50 20 30	
	posterior cingulate gyrus	L	−2 −34 28	
	middle temporal gyrus	L	−30 −42 12	
	cerebellum	R	38 −60 −34	
	cerebellum	L	−34 −62 −34	
	cerebellum	L	−28 −48 −28	
	precuneus	L	−14 −44 52	
8 (1234)	cuneal cortex	L/R	0 −86 26	52.65
	occipital cortex	L	−38 −80 −20	
	frontal eye field	R	6 14 48	
	occipitotemporal area	R	44 −48 −28	
9 (4867)	lingual gyrus	L	−2 −64 8	46.67

To locate and identify the anatomical locations of these clusters, we consulted the Talairach Daemon database (http://www.talairach.org), MRIcron (http://people.cas.sc.edu/rorden/mricron/index.html), and neuroanatomy atlases.

References in the supplemental information

1. S. G. Shamay-Tsoory, J. Aharon-Peretz, D. Perry, Two systems for empathy: a double dissociation between emotional and cognitive empathy in inferior frontal gyrus versus ventromedial prefrontal lesions. *Brain* **132**, 617–627 (2009).
2. T. Singer, C. Lamm, The social neuroscience of empathy. *Ann N Y Acad Sci* **1156**, 81–96 (2009).
3. F. M. Paulus, L. Muller-Pinzler, A. Jansen, V. Gazzola, S. Krach, Mentalizing and the role of the posterior superior temporal sulcus in sharing others' embarrassment. *Cerebral Cortex* **25**, 2065–2075 (2015).
4. C. Lamm, H. Bukowski, G. Silani, From shared to distinct self-other representations in empathy: evidence from neurotypical function and socio-cognitive disorders. *Philos Trans R Soc Lond B Biol Sci* **371** (2016).
5. M. H. Davis, Measuring individual differences in empathy. *Journal of Personality and Social Psychology* **44**, 113–126 (1985).
6. S. Tei *et al.*, Can we predict burnout severity from empathy-related brain activity? *Transl Psychiatry* **4**, e393 (2014).
7. G. J. Taylor, R. M. Bagby, J. D. Parker, The 20-Item Toronto Alexithymia Scale. IV. Reliability and factorial validity in different languages and cultures. *J Psychosom Res* **55**, 277–283 (2003).
8. Y. Moriguchi *et al.*, Empathy and judging other's pain: an fMRI study of alexithymia. *Cereb Cortex* **17**, 2223–2234 (2007).
9. K. Matsuoka, M. Uno, K. Kasai, K. Koyama, Y. Kim, Estimation of premorbid IQ in individuals with Alzheimer's disease using Japanese ideographic script (Kanji) compound words: Japanese version of National Adult Reading Test. *Psychiatry Clin Neurosci* **60**, 332–339 (2006).
10. B. R. Buchsbaum, S. Greer, W. L. Chang, K. F. Berman, Meta-analysis of neuroimaging studies of the Wisconsin card-sorting task and component processes. *Hum Brain Mapp* **25**, 35–45 (2005).
11. S. Tei *et al.*, Collaborative roles of Temporoparietal Junction and Dorsolateral Prefrontal Cortex in Different Types of Behavioural Flexibility. *Sci Rep* **7**, 6415 (2017).
12. K. P. Rankin, J. H. Kramer, B. L. Miller, Patterns of cognitive and emotional empathy in frontotemporal lobar degeneration. *Cogn Behav Neurol* **18**, 28–36 (2005).
13. S. Fukunaga *et al.*, The changes of cognitive function and preoperative cerebral hemodynamics in patients with carotid stenosis following carotid endarterectomy. *West Kyushu J of Rehab Sci* **5**, 7–14 (2012).
14. J. A. Maldjian, P. J. Laurienti, R. A. Kraft, J. H. Burdette, An automated method for neuroanatomic and cytoarchitectonic atlas-based interrogation of fMRI data sets. *Neuroimage* **19**, 1233–1239 (2003).
15. L. Q. Uddin, M. Iacoboni, C. Lange, J. P. Keenan, The self and social cognition: the role of cortical midline structures and mirror neurons. *Trends Cogn Sci* **11**, 153–157 (2007).
16. K. J. Yoder, J. Decety, The Good, the bad, and the just: justice sensitivity predicts neural response during moral evaluation of actions performed by others. *J Neurosci* **34**, 4161–4166 (2014).
17. P. C. Pantelis, L. Byrge, J. M. Tyszka, R. Adolphs, D. P. Kennedy, A specific hypoactivation of right temporo-parietal junction/posterior superior temporal sulcus in response to socially awkward situations in autism. *Soc Cogn Affect Neurosci* **10**, 1348–1356 (2015).
18. H. Takahashi *et al.*, Brain activation associated with evaluative processes of guilt and embarrassment: an fMRI study. *Neuroimage* **23**, 967–974 (2004).
19. M. Bahnemann, I. Dziobek, K. Prehn, I. Wolf, H. R. Heekeren, Sociotopy in the temporoparietal cortex: common versus distinct processes. *Soc Cogn Affect Neurosci* **5**, 48–58 (2010).

20. K. B. Jensen *et al.*, Sharing pain and relief: neural correlates of physicians during treatment of patients. *Mol Psychiatry* **19**, 392–398 (2014).
21. J. P. Kauppi, J. Pajula, J. Niemi, R. Hari, J. Tohka, Functional brain segmentation using inter-subject correlation in fMRI. *Hum Brain Mapp* **38**, 2643–2665 (2017).
22. L. Nummenmaa *et al.*, Emotions promote social interaction by synchronizing brain activity across individuals. *Proc Natl Acad Sci U S A* **109**, 9599–9604 (2012).
23. U. Hasson, Y. Nir, I. Levy, G. Fuhrmann, R. Malach, Intersubject synchronization of cortical activity during natural vision. *Science* **303**, 1634–1640 (2004).
24. E. Simony *et al.*, Dynamic reconfiguration of the default mode network during narrative comprehension. *Nat Commun* **7**, 12141 (2016).
25. C. Bordier, E. Macaluso, Time-resolved detection of stimulus/task-related networks, via clustering of transient intersubject synchronization. *Hum Brain Mapp* **36**, 3404–3425 (2015).
26. S. G. Hofmann, N. Heinrichs, D. A. Moscovitch, The nature and expression of social phobia: toward a new classification. *Clin Psychol Rev* **24**, 769–797 (2004).
27. A. J. Shackman *et al.*, Neural mechanisms underlying heterogeneity in the presentation of anxious temperament. *Proc Natl Acad Sci U S A* **110**, 6145–6150 (2013).
28. M. L. Seghier, C. J. Price, Interpreting and utilising intersubject variability in brain function. *Trends Cogn Sci* **22**, 517–530 (2018).
29. A. G. Huth, W. A. de Heer, T. L. Griffiths, F. E. Theunissen, J. L. Gallant, Natural speech reveals the semantic maps that tile human cerebral cortex. *Nature* **532**, 453–458 (2016).
30. M. Reason *et al.*, Spectators' aesthetic experience of sound and movement in dance performance: A transdisciplinary investigation. *Psychology of Aesthetics, Creativity, and the Arts* **10**, 42 (2016).
31. K. Krishnamoorthy, Y. and Xia, Inferences on correlation coefficients: one-sample, independent and correlated cases. *Journal of Statistical Planning and Inference* **137**, 2362–2379 (2007).
32. Y. Benjamini, Y. Hochberg, Controlling the false discovery rate: a practical and powerful approach to multiple testing. *J. R. Statist. Soc. B* **57**, 289–300 (1995).
33. R. P. Monti, C. Anagnostopoulos, G. & Montana, Learning population and subject-specific brain connectivity networks via mixed neighborhood selection. *The Annals of Applied Statistics* **11**, 2142–2164 (2017).
34. J. Dubois, R. Adolphs, Building a Science of Individual Differences from fMRI. *Trends Cogn Sci* **20**, 425–443 (2016).
35. M. L. Dixon *et al.*, Heterogeneity within the frontoparietal control network and its relationship to the default and dorsal attention networks. *Proc Natl Acad Sci U S A* **115**, E1598–1607 (2018).
36. N. Meinshausen, P. & Bühlmann, High-dimensional graphs and variable selection with the lasso. *The annals of statistics*, 1436–1462 (2006).
37. K. Kelley, Methods for the behavioral, educational, and social sciences: an R package. *Behav Res Methods* **39**, 979–984 (2007).
38. M. Gimenez *et al.*, Altered brain functional connectivity in relation to perception of scrutiny in social anxiety disorder. *Psychiatry Res* **202**, 214–223 (2012).
39. M. N. Servaas *et al.*, Connectomics and neuroticism: an altered functional network organization. *Neuropsychopharmacology* **40**, 296–304 (2015).
40. Y. Ren, V. T. Nguyen, L. Guo, C. C. Guo, Inter-subject functional correlation reveal a hierarchical organization of extrinsic and intrinsic systems in the brain. *Sci Rep* **7**, 10876 (2017).
41. L. Zhe, Bayesian model-averaged regularization for Gaussian graphical models. *Communications in Statistics-Simulation and Computation* **46**, 3213–3223 (2017).